A Stochastic Optimization Approach to Cooperative Building Energy Management via an Energy Hub

Georgios Darivianakis, Angelos Georghiou, Roy S. Smith and John Lygeros

***Abstract*— Building energy management is an active field of research since the potential in energy savings can be substantial. Nevertheless, the opportunities for large savings within individual buildings can be limited by the flexibility of the installed climate control devices and the individual construction characteristics. The energy hub concept allows one to manage a collection of buildings in a cooperative manner, by providing opportunities for load shifting between buildings and the sharing of expensive but energy efficient equipment housed in the hub, such as heat pumps, boilers, batteries. Typically, control design for the buildings and the energy hub are done separately, underutilizing the potential flexibility provided by the interconnected system. To address these issues, we propose a unified framework for controlling the operation of the energy hub and the buildings it connects to. By modeling all exogenous disturbance parameters as stochastic processes, and by using state-space representation of the building dynamics, we formulate a multistage stochastic optimization problem to minimize the total energy consumption of the system in a cooperative manner. We solve the resulting infinite dimensional optimization problem using a decision rule approximation, and we benchmark its performance on a numerical study, comparing it with established solution techniques.**

I. Introduction

Recent studies [1], [2] have shown that around three quarters of the total electricity consumption in Europe and the US is attributed to buildings, with almost half of the energy being used for the building's climate control. In addition, European standards require office buildings to maintain their room temperature within given ranges (typically 21°C to 25°C) during working hours, with only minor violations during the course of a year [3]. Therefore, substantial efforts have been devoted to the optimal control of climate control devices to reduce their impact on electricity consumption [4]–[6].

To reach further savings, economies of scales need to be exploited. This can be achieved in two ways: (i) Office building aggregation provides the opportunity to manage collectively their energy needs, taking advantage of the intra-day price fluctuations in the electricity price and performing efficient load shifting between buildings; (ii) Sharing the use of energy efficient equipment such as heat pumps, boilers, batteries, as well photovoltics, which are usually prohibitively expensive to be purchased and operated by a single building unit. The concept of the *energy hub* serves this dual purpose by housing the expensive components shared between buildings and provides the interface between the building community and the energy grid [7].

The energy hub idea is a rather recent concept, with the main body of the literature separating the optimal control of the energy hub and the buildings connected to the system. Indeed, a number of papers treats the building energy demands as exogenous signals, which are typically estimated using building simulation environments such as the EnergyPlus [8]. These models include both deterministic [9] and stochastic [10] formulations, and aim to optimally control the devices within the energy hub. More complex systems with multiple energy hubs also appear in the literature, where deterministic model predictive control approaches are used for the optimal operation of the system [11]. The downside of decoupling the operation of the energy hub and the interconnected buildings, is the underutilization of the load shifting capabilities of the buildings in the interconnected system and the suboptimal operation of the devices present in the energy hub.

The goal of this is paper is to present a unified framework for controlling the operation of the energy hub and the buildings it connects to. The proposed methodology minimizes the total energy consumption of the building community in a cooperative fashion. To this end, we consider the stochastic state-space representation for the building dynamics proposed in [12] and formulate a stochastic state-space models for the devices present in the energy hub base on the work of [9], [13], [14]. We use modern robust optimization techniques known as *decision rules*, [15], [16] for approximating the resulting multistage stochastic optimization problem, and we compare our results to traditional deterministic and robust optimization techniques.

The paper is organised as follows. In Section II we present the model description for the underlying system, and in Section III we formulate the resulting optimization problem. The decision rules solution method is summarized in Section IV and in Section V we present our computational results.

Notation: All random vectors appearing in this paper are defined on an abstract probability space $(\Omega, \mathcal{F}, \mathbb{P})$, where $\mathbb{E}(\cdot)$ denotes the expectation operator with respect to $\mathbb{P}$. Random vectors are represented in boldface. For any random vector $\boldsymbol{\xi}$, we let $\sigma(\boldsymbol{\xi})$ be the σ-algebra of $\mathcal{F}$ generated by $\boldsymbol{\xi}$, while $\mathcal{L}^2(\boldsymbol{\xi}) = \mathcal{L}^2(\Omega, \sigma(\boldsymbol{\xi}), \mathbb{P})$ denotes the space of all $\sigma(\boldsymbol{\xi})$-measurable square-integrable random variables. *All equalities and inequalities involving random variables are assumed to hold with probability 1.* Finally, $\boldsymbol{e}$ denotes the vector of ones and its size will be clear from the context.

This research was partially funded by CTI within the SCCER FEEB&D (contract no. 1155000149), the Swiss National Science Foundation under the project IMES and the European Commission under the project Local4Global.

The authors are with the Automatic Control Laboratory, Department of Electrical Engineering and Information Technology, ETH Zurich, 8092 Zurich, Switzerland. {gdarivia, angelosg, rsmith, lygeros}@control.ee.ethz.ch

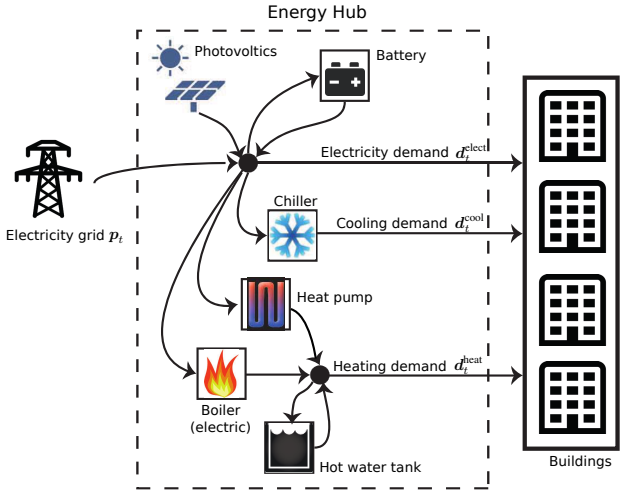

Fig. 1. District electricity, heating and cooling network.

II. Model description

In this section, we use the illustrative example depicted in Fig. 1 to descibe the governing dynamics of the underlying system. The system can be described by a discrete time, bi-linear model, in which the dynamics are affected by stochastic exogenous disturbances. We assume that these disturbances evolve according to given stochastic processes $\{\boldsymbol{\xi}_t\}_{t\in\mathcal{T}}$, where $\mathcal{T} = \{1,\dots,T\}$, and T is the length of the horizon considered with an hourly time discretization. Here, the vector $\boldsymbol{\xi}_t$ encompasses all stochastic processes that appear in the problem, including the stochastic evolution of the temperature, solar radiation and internal gains of the buildings. We also denote by $\boldsymbol{I}_t$ the information basis for the operating decisions taken at stage t. The structure of $\boldsymbol{I}_t$ will dictate the behaviour of the corresponding operating decisions; in principle it can contain any information that is relevant to devices at decision time t. This can include the full or a partial history of the stochastic processes $\boldsymbol{\xi}_t$ as well as forecasts of some future states of the stochastic processes. Note that all quantities appearing in the paper are real numbers, with the size of the corresponding vectors will be clear from the context.

A. Structure of the system

The system comprises a set of buildings, denoted by $\mathcal{B}$, and an energy hub. The buildings meet all their energy requirements from the energy hub. At time t, each building $i \in \mathcal{B}$ can have three energy demand requirements: (i) demand for electricity $\boldsymbol{d}_{t,i}^{\text{elect}} \in \mathcal{L}^2(\boldsymbol{I}_t)$, (ii) demand for heating $\boldsymbol{d}_{t,i}^{\text{heat}} \in \mathcal{L}^2(\boldsymbol{I}_t)$, and (iii) demand for cooling $\boldsymbol{d}_{t,i}^{\text{cool}} \in \mathcal{L}^2(\boldsymbol{I}_t)$. Note that $\{\boldsymbol{d}_{t,i}^{\text{elect}}\}_{t\in\mathcal{T}}$, $\{\boldsymbol{d}_{t,i}^{\text{heat}}\}_{t\in\mathcal{T}}$, $\{\boldsymbol{d}_{t,i}^{\text{cool}}\}_{t\in\mathcal{T}}$ are in fact stochastic processes which are affected by exogenous stochastic process $\{\boldsymbol{\xi}_t\}_{t\in\mathcal{T}}$. We denote the energy purchased by the energy hub from the grid at time t by $\boldsymbol{p}_t \in \mathcal{L}^2(\boldsymbol{I}_t)$.

B. Energy hub dynamics

In the following, we denote by $\mathcal{D}$ the set of devices controlled by the energy hub. The following dynamical system describes the evolution of energy $\boldsymbol{x}_{t,i}$ in a particular device $i \in \mathcal{D}$:

$$\left.\begin{aligned} \boldsymbol{x}_{t+1,i} = A_i\boldsymbol{x}_{t,i} + B_i^{\text{in}}\boldsymbol{u}_{t,i}^{\text{in}} + B_i^{\text{out}}\boldsymbol{u}_{t,i}^{\text{out}} + C_i\boldsymbol{\xi}_t, \\ (\boldsymbol{x}_{t,i}, \boldsymbol{u}_{t,i}^{\text{in}}, \boldsymbol{u}_{t,i}^{\text{out}}, \boldsymbol{\xi}_t) \in \mathcal{C}_{t,i}, \\ \boldsymbol{u}_{t,i}^{\text{in}},\ \boldsymbol{u}_{t,i}^{\text{out}} \in \mathcal{L}^2(\boldsymbol{I}_t), \end{aligned}\right\} \forall t \in \mathcal{T}. \tag{1}$$

Here, $\boldsymbol{u}_{t,i}^{\text{in}}$ and $\boldsymbol{u}_{t,i}^{\text{out}}$ are the controlled inputs and outputs of energy from the device, respectively. Set $\mathcal{C}_{t,i}$ describes state and input constraints for device i.

The three energy carriers (electrical, heating, cooling) give rise to three energy balancing constraints. The electricity balancing constraint is given by

$$\boldsymbol{p}_t + \sum_{i\in \text{E}_+} \boldsymbol{u}_{t,i}^{\text{out}} = \sum_{i\in \text{E}_-} \boldsymbol{u}_{t,i}^{\text{in}} + \sum_{i\in\mathcal{B}} \boldsymbol{d}_{t,i}^{\text{elect}}, \quad \forall t \in \mathcal{T}, \tag{2a}$$

where $\text{E}_+ \subseteq \mathcal{D}$ and $\text{E}_- \subseteq \mathcal{D}$ are the set of devices that can contribute and consume electricity, respectively, within the energy hub. In the example depicted in Figure 1, $\text{E}_+ = \{\text{photovoltaics, battery}\}$ and $\text{E}_- = \{\text{heat pump, chiller, boiler, battery}\}$. The heating energy balancing constraint is given by

$$\sum_{i\in \text{H}_+} \boldsymbol{u}_{t,i}^{\text{out}} = \sum_{i\in \text{H}_-} \boldsymbol{u}_{t,i}^{\text{in}} + \sum_{i\in\mathcal{B}} \boldsymbol{d}_{t,i}^{\text{heat}}, \quad \forall t \in \mathcal{T}, \tag{2b}$$

where $H_+ \subseteq \mathcal{D}$ and $H_- \subseteq \mathcal{D}$ are the set of devices that can contribute and consume heat energy, respectively, within the energy hub. In Figure 1, these sets are defined as $\text{H}_+ = \{\text{heat pump, boiler, hot water tank}\}$ and $\text{H}_- = \{\text{hot water tank}\}$. Finally, the cooling energy balancing constraint is as follows

$$\sum_{i\in C_+} \boldsymbol{u}_{t,i}^{\text{out}} = \sum_{i\in\mathcal{B}} \boldsymbol{d}_{t,i}^{\text{cool}}, \quad \forall t \in \mathcal{T}, \tag{2c}$$

with $C_+ \subseteq \mathcal{D}$, and $C_+ = \{\text{chiller}\}$ in our running example.

We close this section by defining the following constraint set for the energy hub:

$$\text{EH} := \Big\{ \{\boldsymbol{p}_t\}_{t\in\mathcal{T}}, \{\boldsymbol{d}_t\}_{t\in\mathcal{T}} : \exists \{\boldsymbol{u}_t^{\text{in}}\}_{t\in\mathcal{T}}, \{\boldsymbol{u}_t^{\text{out}}\}_{t\in\mathcal{T}} \text{ such that (1), (2) hold} \Big\}.$$

where $\boldsymbol{d}_t = (\boldsymbol{d}_t^{\text{elect}}, \boldsymbol{d}_t^{\text{heat}}, \boldsymbol{d}_t^{\text{cool}})$, $\boldsymbol{u}_t^{\text{in}} = (\boldsymbol{u}_{t,1}^{\text{in}}, \dots, \boldsymbol{u}_{t,|\mathcal{D}|}^{\text{in}})$ and $\boldsymbol{u}_t^{\text{out}} = (\boldsymbol{u}_{t,1}^{\text{out}}, \dots, \boldsymbol{u}_{t,|\mathcal{D}|}^{\text{out}})$.

C. Building dynamics

We use the building model developed in [12] which gives rise to a bi-linear state-space model. The model captures the evolution of temperature in the building and has as states the temperatures of the individual rooms, walls, floors and ceiling layers of the building, and as control inputs the energy provided by the radiators, blinds position, air handling units (AHU) and thermally activated building structures (TABS). Models of this type can be developed using capacitance-resistance model of the building and their accuracy was benchmarked against established building simulation software such as EnergyPlus [8] and validated against real

buildings [17]. For each building $i \in \mathcal{B}$ and time point $t \in \mathcal{T}$, the bi-linear dynamic are given by:

$$\begin{aligned} \boldsymbol{x}_{t+1,i} = A_i \boldsymbol{x}_{t,i} + B_i \boldsymbol{u}_{t,i} + C_i \boldsymbol{\xi}_t \\ + \sum_{j \in \mathcal{D}_i^{\mathrm{b}}} \left(D_{i,j} \boldsymbol{\xi}_t + E_{i,j} \boldsymbol{x}_{t,i}\right) \boldsymbol{u}_{t,i,j}, \\ (\boldsymbol{u}_i, \boldsymbol{\xi}) \in \mathcal{U}_i,\ \boldsymbol{u}_{t,i} \in \mathcal{L}^2(\boldsymbol{I}_t), \end{aligned} \tag{3a}$$

where $\mathcal{D}_i^{\mathrm{b}} = \{\text{radiators, blinds position, AHU, TABS}\}$ is the set of devices present in the building. The units of states $\boldsymbol{x}_{t,i}$ are in degrees Celsius. $\mathcal{U}_i$ is the set of linear coupling constraints between inputs and disturbances. We define $\boldsymbol{x}_{t,i}^{\text{room}}$ to be the subvector of $\boldsymbol{x}_{t,i}$ which denotes the states associated with room temperatures in the building. The following constraints ensure that the temperature in the rooms $\boldsymbol{x}_{t,i}^{\text{room}}$ remain within user comfort ranges:

$$\mathrm{lb}_{t,i} \leq \boldsymbol{x}_{t,i}^{\text{room}} \leq \mathrm{ub}_{t,i}, \quad \forall t \in \mathcal{T}, \tag{3b}$$

where $\mathrm{lb}_{t,i}$ and $\mathrm{ub}_{t,i}$ are lower and upper bounds on the room temperature at time t and building i. We will refer to constraint set (3b) as the *comfort constraints*. We emphasize that these ranges are time varying as rooms might have different temperature requirements between day and night hours.

Each building device is categorised in terms of the source of energy it consumes. Note that the TABS inject both heating and cooling within certain layers of the building structure. Therefore, for each building $i \in \mathcal{B}$, we can formulate the energy balance constraints as follows:

$$\left.\begin{aligned} \boldsymbol{d}_{t,i}^{\text{elect}} &= \boldsymbol{e}^\top \boldsymbol{u}_{t,i,\text{AHU}}, \\ \boldsymbol{d}_{t,i}^{\text{heat}} &= \boldsymbol{e}^\top \boldsymbol{u}_{t,i,\text{radiator}} + \boldsymbol{e}^\top \boldsymbol{u}_{t,i,\text{TABS}}, \\ \boldsymbol{d}_{t,i}^{\text{cool}} &= \boldsymbol{e}^\top \boldsymbol{u}_{t,i,\text{TABS}}, \end{aligned}\right\} \quad \forall t \in \mathcal{T}. \tag{4}$$

We close this section by defining the following constraint set for each building $i \in \mathcal{B}$:

$$\mathrm{B}_i := \left\{ \{\boldsymbol{d}_{t,i}\}_{t \in \mathcal{T}} : \exists \{\boldsymbol{u}_{t,i}\}_{t \in \mathcal{T}} \text{ such that (3), (4) hold} \right\} \tag{5}$$

where

$$\begin{aligned} \boldsymbol{d}_{t,i} &= (\boldsymbol{d}_{t,i}^{\text{elect}}, \boldsymbol{d}_{t,i}^{\text{heat}}, \boldsymbol{d}_{t,i}^{\text{cool}}), \\ \boldsymbol{u}_{t,i} &= (\boldsymbol{u}_{t,i,1}, \ldots, \boldsymbol{u}_{t,i,|\mathcal{D}_i^{\mathrm{b}}|}). \end{aligned}$$

D. Disturbance modeling

We model the disturbance $\boldsymbol{\xi}_t$ as a known deterministic forecast f_t, plus a random error $\boldsymbol{\epsilon}_t$ which we assume is a stochastic process, evolving with a known distribution. We assume that $\boldsymbol{\epsilon}_t \in [\underline{\mathrm{eb}}_t, \overline{\mathrm{eb}}_t]$, where $\underline{\mathrm{eb}}_t$ and $\overline{\mathrm{eb}}_t$ are the error lower and upper bounds, respectively. Moreover, we assume that the error terms are coupled in time. In particular, we assume that $\boldsymbol{\epsilon}_{t+1} - \boldsymbol{\epsilon}_t \in [\underline{\mathrm{db}}_t, \overline{\mathrm{db}}_t]$, $t = 1, \ldots, T-1$, where $\underline{\mathrm{db}}_t$ and $\overline{\mathrm{db}}_t$ are the time deviation lower and upper bounds, respectively. Imposing the temporal structure on vector $\boldsymbol{\xi} = (\boldsymbol{\xi}_1, \ldots, \boldsymbol{\xi}_T)$ with $\boldsymbol{\xi} \in \mathbb{R}^{k_t}$ and $k = \sum_{t \in \mathcal{T}} k_t$, the uncertainty set for the stochastic process $\{\boldsymbol{\xi}_t\}_{t \in \mathcal{T}}$ can be written as follows:

$$\Xi = \left\{ \begin{aligned} \boldsymbol{\xi} \in \mathbb{R}^k : \exists\, \boldsymbol{\epsilon}_t \in \mathbb{R}^{k_t},\ \boldsymbol{\xi}_t &= f_t + \boldsymbol{\epsilon}_t, t \in \mathcal{T}, \\ \boldsymbol{\epsilon}_t \in [\underline{\mathrm{eb}}_t, \overline{\mathrm{eb}}_t], &\quad t \in \mathcal{T}, \\ \boldsymbol{\epsilon}_{t+1} - \boldsymbol{\epsilon}_t \in [\underline{\mathrm{db}}_t, \overline{\mathrm{db}}_t], &\quad t \in \mathcal{T} \backslash \{T\} \end{aligned} \right\}.$$

Note that in this definition of Ξ, each pair of elements $\boldsymbol{\xi}_{t,i}$ and $\boldsymbol{\xi}_{t,j}$, $i \neq j$, are assumed to be independent. In general, this assumption can be lifted by enriching Ξ with additional constraints, capturing the correlations between the different random variables.

III. Optimization problem

The goal of the building community is to minimize the total expected costs with respect to the electricity purchased from the grid, over a finite horizon. This must be achieved while satisfying the comfort constraint and operational constraints of the devices in the system. We assume that the cost of electricity at time t is known, and is denoted by c_t. Starting with initial conditions $\boldsymbol{x}_1 = x_1$, where x_1 is the vector containing the initial states for both the dynamical systems in the energy hub and buildings, the problem can be formulated as a multistage, bi-linear, stochastic optimization problem,

$$\begin{aligned} J(x_1) = \min\ & \mathbb{E}\left(\sum_{t \in \mathcal{T}} c_t \boldsymbol{p}_t\right) \\ \text{s.t. } & \boldsymbol{p}_t \in \mathcal{L}^2(\boldsymbol{I}_t),\ \boldsymbol{d}_{t,i} \in \mathcal{L}^2(\boldsymbol{I}_t),\ \forall t \in \mathcal{T},\ i \in \mathcal{B}, \\ & \left(\{\boldsymbol{p}_t\}_{t \in \mathcal{T}}, \{\boldsymbol{d}_t\}_{t \in \mathcal{T}}\right) \in \mathrm{EH}, \\ & \{\boldsymbol{d}_{t,i}\}_{t \in \mathcal{T}} \in \mathrm{B}_i,\ \forall i \in \mathcal{B}. \end{aligned} \tag{6}$$

Problem (6) is in general computationally intractable, mainly due to the non-linear dynamics in (3a). In addition, Problem (6) might be infeasible for some initial conditions. We now address these drawbacks by defining an approximation of constraint set (3) to obtain a linear multistage stochastic optimization problem. A linearized version of the bi-linear dynamics in (3a) is as follows:

$$\begin{aligned} \boldsymbol{x}_{t+1,i} = A_i \boldsymbol{x}_{t,i} + B_i \boldsymbol{u}_{t,i} + C_i \boldsymbol{\xi}_t \\ + \sum_{j \in \mathcal{D}_i^{b}} \left(D_{i,j} \mathbb{E}(\boldsymbol{\xi}_t) + E_{i,j} x_{1,i}\right) \boldsymbol{u}_{t,i,j}, \\ (\boldsymbol{u}_i, \boldsymbol{\xi}) \in \mathcal{U}_i,\ \boldsymbol{u}_{t,i} \in \mathcal{L}^2(\boldsymbol{I}_t). \end{aligned} \tag{7a}$$

In particular, the bilinear terms $\boldsymbol{x}_{t,i}\boldsymbol{u}_{t,i,j}$ and $\boldsymbol{\xi}_{t,i}\boldsymbol{u}_{t,i,j}$ in (3a) are now replace with the linear terms $x_{1,i}\boldsymbol{u}_{t,i,j}$ and $\mathbb{E}(\boldsymbol{\xi}_t)\boldsymbol{u}_{t,i,j}$, respectively, where $x_{1,i}$ is the initial condition for the state of building i, and $\mathbb{E}(\boldsymbol{\xi}_t)$ denotes the expected value of $\boldsymbol{\xi}_t$. To address infeasible instances of Problem (6), we define a soft constraint formulation of the comfort constraints (3b) as follows:

$$\left.\begin{aligned} \max\{\mathrm{lb}_{t,i} - \boldsymbol{x}_{t,i}^{\text{room}}, 0, \boldsymbol{x}_{t,i}^{\text{room}} - \mathrm{ub}_{t,i}\} \leq \boldsymbol{s}_{t,i}. \\ \boldsymbol{s}_{t,i} \in \mathcal{L}^2(\boldsymbol{I}_t). \end{aligned}\right\} \quad \forall t \in \mathcal{T}, \tag{7b}$$

where $\boldsymbol{s}_{t,i}$ are slack variables. If the $\mathbb{E}(\boldsymbol{s}_{t,i}) = 0$, then constraints (7b) reduce to constraints (3b). If $\mathbb{E}(\boldsymbol{s}_{t,i}) > 0$, then the (3b) can be violated for some realization of $\boldsymbol{\xi}_t$. We remark that in general infeasibility may be an issue also for the energy hub constraints EH. In this case, a similar relaxation can also be applied for the constraint in EH. In the following, we assume EH is not empty for all initial

conditions $\boldsymbol{x}_1 = x_1$. The linearized version of constraint set (5) is:

$$\widehat{\mathrm{B}}_i := \Big\{ \{\boldsymbol{d}_{t,i}\}_{t\in\mathcal{T}},\, \{\boldsymbol{s}_{t,i}\}_{t\in\mathcal{T}} \,:\, \exists \{\boldsymbol{u}_{t,i}\}_{t\in\mathcal{T}} \text{ such that (4), (7) hold} \Big\}.$$

The linearized variant of Problem (6) is given as follows:

$$\begin{aligned} J(x_1) = \min\, & \mathbb{E}\left(\sum_{t\in\mathcal{T}} c_t \boldsymbol{p}_t + \gamma \sum_{t\in\mathcal{T}} \sum_{i\in\mathcal{B}} \boldsymbol{e}^\top \boldsymbol{s}_{t,i} \right) \\ \text{s.t. } & \boldsymbol{p}_t \in \mathcal{L}^2(\boldsymbol{I}_t),\, \boldsymbol{d}_{t,i} \in \mathcal{L}^2(\boldsymbol{I}_t), \forall i \in \mathcal{B},\, t \in \mathcal{T}, \\ & \boldsymbol{s}_{t,i} \in \mathcal{L}^2(\boldsymbol{I}_t),\ \forall i \in \mathcal{B},\, t \in \mathcal{T}, \\ & \big(\{\boldsymbol{p}_t\}_{t\in\mathcal{T}}, \{\boldsymbol{d}_t\}_{t\in\mathcal{T}}\big) \in \mathrm{EH}, \\ & \big(\{\boldsymbol{d}_{t,i}\}_{t\in\mathcal{T}}, \{\boldsymbol{s}_{t,i}\}_{t\in\mathcal{T}}\big) \in \widehat{\mathrm{B}}_i,\ \forall i \in \mathcal{B}. \end{aligned} \tag{8}$$

The additional term $\gamma \sum_{t\in\mathcal{T}} \sum_{i\in\mathcal{B}} \boldsymbol{e}^\top \boldsymbol{s}_{t,i}$ in the objective penalizes constraint violations for the constraint set (7b), with parameter $\gamma \in \mathbb{R}_+$ providing the tradeoff between energy bought from the grid and the amount of room temperature violations. Problem (8) still retains its infinite structure involving a continuum space of decision variables and constraints. However, by taking advantage of the linear structure of the constraints and objective, in the next section we will employ well established approximation techniques which will result to finite dimensional, linear optimization problems.

IV. Solution method

We now simplify the infinite dimensional structure of Problem (8) by restricting the infinite space of the recourse decisions $\boldsymbol{p}_t$, $\boldsymbol{d}_{t,i}$, $\boldsymbol{s}_{t,i}$ to admit a linear structure with respect to their corresponding information vector I_t. This is typically referred to the *linear decision rule approximation*. In this setting, the structure of a policy, say $\boldsymbol{p}_t \in \mathcal{L}^2(\boldsymbol{I}_t)$, is approximated by $\boldsymbol{p}_t = p_t^\top \boldsymbol{I}_t$, where $p_t \in \mathbb{R}^{|I_t|}$. If $\boldsymbol{I}_t = (1, \boldsymbol{\xi}_1, \ldots, \boldsymbol{\xi}_{t-1})^\top \in \mathbb{R}^t$, then the structure of $\boldsymbol{p}_t$ reduces to the strictly causal *affine policy* $\boldsymbol{p}_t = p_{t,0} + \sum_{s=1}^{t-1} p_{t,s} \boldsymbol{\xi}_s$. If, however, the information vector is deterministically known, e.g., $\boldsymbol{I}_t = (1) \in \mathbb{R}$, then $\boldsymbol{p}_t$ reduces to the *open-loop policy* $\boldsymbol{p}_t = p_t$. Applying linear decision rules to all recourse decisions in Problem (8), gives rise to the following optimization problem.

$$\begin{aligned} J(x_1) = \min\, & \mathbb{E}\left(\sum_{t\in\mathcal{T}} c_t p_t^\top \boldsymbol{I}_t + \gamma \sum_{t\in\mathcal{T}} \sum_{i\in\mathcal{B}} \boldsymbol{e}^\top S_{t,i}^\top \boldsymbol{I}_t \right) \\ \text{s.t. } & p_t \in \mathbb{R}^{|I_t|},\ \forall t \in \mathcal{T}, \\ & d_{t,i}^{\text{elect}}, d_{t,i}^{\text{heat}}, d_{t,i}^{\text{cool}} \in \mathbb{R}^{|I_t|},\ \forall i \in \mathcal{B},\, t \in \mathcal{T}, \\ & S_{t,i} \in \mathbb{R}^{|\text{rooms}|_i \times |I_t|},\ \forall i \in \mathcal{B},\, t \in \mathcal{T}, \\ & \big(\{p_t^\top \boldsymbol{I}_t\}_{t\in\mathcal{T}}, \{D_t \boldsymbol{I}_t\}_{t\in\mathcal{T}}\big) \in \mathrm{EH}, \\ & \big(\{D_{t,i} \boldsymbol{I}_t\}_{t\in\mathcal{T}}, \{S_{t,i} \boldsymbol{I}_t\}_{t\in\mathcal{T}}\big) \in \widehat{\mathrm{B}}_i,\ \forall i \in \mathcal{B}, \end{aligned} \tag{9}$$

where

$$D_t = \begin{pmatrix} D_{t,1} \\ \vdots \\ D_{t,|\mathcal{B}|} \end{pmatrix},\ D_{t,i} = \begin{pmatrix} d_{t,i}^{\text{elect}\top} \\ d_{t,i}^{\text{heat}\top} \\ d_{t,i}^{\text{cool}\top} \end{pmatrix}.$$

Problem (9) has a semi-infinite structure since it involves a finite number of decision variables p_t, D_t, S_t, $t \in \mathcal{T}$, and an infinite number of constraints due to the requirement that the constraints in EH and $\widehat{\mathrm{B}}_i$ must hold with probability 1. Note that since all constraints are linear both with respect to the decision variables and $\boldsymbol{\xi}$, this reduces to the robust constraints that need to hold for all $\boldsymbol{\xi} \in \Xi$. Therefore, by employing linear programming duality, [15], [18], the semi-infinite constraint system can be reexpressed in terms of a finite number of linear constraints. We emphasize that the expected values of the information sets $\mathbb{E}(\boldsymbol{I}_t)$ can be evaluated since we assume that the distribution of the random variables $\boldsymbol{\xi}_t$ is given.

Another common approximation used in practice is to replace all random variables in Problem (8) with their expected value. This deterministic problem, sometimes referred to as the *certainty equivalence problem*, results in a highly scalable solution method, but does not necessarily guarantee robust constraint satisfaction. In the following section, we apply the adaptive and open-loop policies to instances of Problem (8) and compare their performance against the certainty equivalence solution method.

V. Numerical results

In this section, we consider a problem with 7 sources of disturbance: ambient and ground temperatures, four sources of solar radiation (North, South, East, West), and building internal gains. Historical weather and occupancy data were collected in an experimantal building study [17]. At each time point, and for each uncertain quantity, the data consist of a forecast f_s and a realization trajectory r_s, $s = 1, \ldots, N$, with $f_{s,t}$ denoting the forecast of stage t starting from stage s, and corresponding realization denoted by $r_{s,t}$. Remembering that in the definition Ξ, $\boldsymbol{\epsilon}_t$ denotes the error deviation from the forecast starting at time $s = 1$, the finite scenario realizations of $\boldsymbol{\epsilon}_t$ are constructed as follows:

$$\epsilon_{t,s} = r_{s,t} - f_{s,t},\ \forall s = 1, \ldots, N,\, t \in \mathcal{T},$$

with the error bounds being $\underline{\text{eb}}_t = \min\{\epsilon_{t,1}, \ldots, \epsilon_{t,N}\}$ and $\overline{\text{eb}}_t = \max\{\epsilon_{t,1}, \ldots, \epsilon_{t,N}\}$, and time deviation bounds being $\underline{\text{db}}_t = \min\{\epsilon_{t+1,1} - \epsilon_{t,1}, \ldots, \epsilon_{t+1,N} - \epsilon_{t,N}\}$ and $\overline{\text{db}}_t = \max\{\epsilon_{t+1,1} - \epsilon_{t,1}, \ldots, \epsilon_{t+1,N} - \epsilon_{t,N}\}$. Moreover, we assume that the stochastic process ϵ_t, evolves according to the empirical distribution which is constructed using the historical data.

We consider an energy hub comprising 5 devices: chiller, boiler, heat pump (HP), photovoltaics (PV) and battery. We model the chiller, boiler and heat pump using a coefficient of performance [9], which gives rise to the following constraints.

$$\left.\begin{aligned} \boldsymbol{u}_{t,\text{chiller}}^{\text{out}} &= 0.7 \boldsymbol{u}_{t,\text{chiller}}^{\text{in}}, \\ \boldsymbol{u}_{t,\text{boiler}}^{\text{out}} &= 0.7 \boldsymbol{u}_{t,\text{boiler}}^{\text{in}}, \\ \boldsymbol{u}_{t,\text{HP}}^{\text{out}} &= 3 \boldsymbol{u}_{t,\text{HP}}^{\text{in}}, \end{aligned}\right\} \quad \forall t \in \mathcal{T}.$$

Building specifications

No.	Area(m^2)	WFA	BT	CT	Input Devices
1	420	30%	SP	heavy	AHU, blinds, radiator
2	228	50%	SP	light	AHU, blinds, TABS
3	276	80%	SA	light	AHU, blinds, TABS
4	516	50%	SA	heavy	AHU, blinds, radiator
5	324	50%	SP	heavy	AHU, blinds, radiator

TABLE I

SUMMARY OF THE 5 BUILDINGS USED IN THE SIMULATIONS.

All three devices are assumed to have infinite capacity, with $\boldsymbol{u}_t^{\text{in}}, \boldsymbol{u}_t^{\text{out}} \geq 0$ for all $t \in \mathcal{T}$. We consider a photovoltaic array with maximum output of 8.02kW, which is modelled using the following linear constraints [13] that depend linearly on the ambient temperature, and the solar radiation (South):

$$0 \leq \boldsymbol{u}_{t,\text{PV}}^{\text{out}} \leq 0.1655 - 0.0066\boldsymbol{\xi}_{t,\text{Amb.Temp.}} + 7.8\boldsymbol{\xi}_{t,\text{Solar(S)}},$$

for all $t \in \mathcal{T}$. Note that the units of $\boldsymbol{\xi}_{t,\text{Solar(S)}}$ are measured in kW/m^2 and can typically take values $\boldsymbol{\xi}_{t,\text{Solar(S)}} \in [0, 1]$. Finally, we consider a lead-acid battery [14], with a 5kW capacity, giving rise to the following linear dynamical system:

$$\begin{aligned}\boldsymbol{x}_{t+1} = &\begin{pmatrix}0.51 & 0.22\\ 0.47 & 0.78\end{pmatrix}\boldsymbol{x}_t \\ &+ \begin{pmatrix}0.61\\ 0.25\end{pmatrix}\boldsymbol{u}_t^{\text{in}} + \begin{pmatrix}-0.83\\ -0.39\end{pmatrix}\boldsymbol{u}_t^{\text{out}},\end{aligned} \quad \forall t \in \mathcal{T},$$

where the states and control are constrained by:

$$\left.\begin{array}{l} 0 \leq \boldsymbol{u}_t^{\text{in}},\, \boldsymbol{u}_t^{\text{out}} \leq 8, \\ 1 \leq \boldsymbol{x}_{t,1} + \boldsymbol{x}_{t,2} \leq 5,\, \boldsymbol{x}_t \geq 0, \\ 0.62\boldsymbol{x}_{t,1} + 0.27\boldsymbol{x}_{t,2} - \boldsymbol{u}_t^{\text{out}} \geq 0, \\ 0.84\boldsymbol{x}_{t,1} + 0.37\boldsymbol{x}_{t,2} + \boldsymbol{u}_t^{\text{in}} \leq 2.58, \\ 0.73\boldsymbol{x}_{t,1} + 0.73\boldsymbol{x}_{t,2} + \boldsymbol{u}_t^{\text{in}} \leq 3.66. \end{array}\right\} \quad \forall t \in \mathcal{T}.$$

The dynamics and constraints of each building, given in (3), are generated using the BRCM toolbox [12]. In particular, we use building models described in [17], with their main features summarised in Table I. Each building is characterised by the building type BT $\in$ {Swiss Passive (SP), Swiss Average(SA)}, and construction type CT = {heavy, light}. Moreover, each building is decomposed into zones, which are characterized by a window fraction area WFA = $\{30\%, 50\%, 80\%\}$ and their corresponding facade orientation.

Time	c_t	lb_t	ub_t
05:00 - 23:00	0.145CHF	21°C	25°C
23:00 - 05:00	0.097CHF	15°C	30°C

TABLE II

ELECTRICITY DAY/NIGHT TARIFF VARIATIONS AND COMFORT CONSTRAINTS BOUNDS.

The following computation experiments compare the performance of affine decision rules (ADR), open-loop policies (OLP) and the certainty equivalent problem (CEP), for a problem instance with $T = 12$, $\gamma = 10^3$. All problems assume time-varying electricity tariffs and comfort constraints given in Table II. Note that the electricity prices c_t, are given in Swiss Franc (CHF) and the same comfort bounds lb_t, ub_t are used in all rooms and all buildings considered in the system. The performance of the system is evaluated on a receding horizon implementation of the system, i.e., the first input resulting from the corresponding approximation of Problem (9) together with the disturbance realizations are applied to the *original nonlinear system dynamics* (3a), and the next state is evaluated. The procedure is repeated in a receding horizon fashion for a time horizon of 1 week. The system was simulated using data realizations of 8 consecutive weeks (restarting at the beginning of each week) for the winter and summer periods of 2007, starting January 1st and June 29th, respectively. Table III reports the statistics from these simulation results, with the cost being measured in Swiss Francs (CHF) and comfort constraint violations measured in Kelvin hours (Kh), and the entries correspond to (mean,standard deviation) over the scenarios considered.

Winter

Method	Energy Purchased (CHF)	Violations per Zone (Kh)
CEP	$(392.96, 6.69)$	$(3.21, 0.23)$
OLP	$(452.75, 4.84)$	$(0.59, 0.14)$
ADR	$(425.52, 6.17)$	$(0.52, 0.14)$

Summer

Method	Energy Purchased (CHF)	Violations per Zone (Kh)
CEP	$(30.20, 2.13)$	$(1.2, 0.09)$
OLP	$(53.74, 2.87)$	$(0.43, 0.06)$
ADR	$(48.64, 3.07)$	$(0.23, 0.04)$

TABLE III

RECEDING HORIZON SIMULATIONS.

We observe that the certainty equivalent approximation produces the least cost at the expense of large constraint violations both for the winter and summer periods. The robust approximations (open-loop and affine policies), produce higher costs but with much lower constraint violation. The poor performance of the certainty equivalent approximation with respect to the constraint violation can be explained in two ways: (i) the approximation assumes a deterministic evolution of the uncertain parameters, which results in frequent constraint violations since the system pushes the states close to the comfort constraints in order to minimize the electricity cost, however, when an unaccounted disturbance is realized, the next state ends up being outside the comfort constraints. Moreover, the model mismatch between the linear dynamics (7a) and the actual bi-linear dynamics (3a), reduce the predictive capabilities of Problem (8). In contrast, the robust approximations fully incorporate the stochastic evolution of uncertain parameters but suffer slightly from the linearization of the system dynamics. We note that the slightly more constraint violations of the open-loop polices compared to affine decision rules can be attributed to the non-adaptive nature of the open-loop policies. The inability of open-loop policies to adapt can potentially lead to greater difficulty in satisfying the robust constraints and thus lead to undesired constraint violations. Finally, for each step in the receding

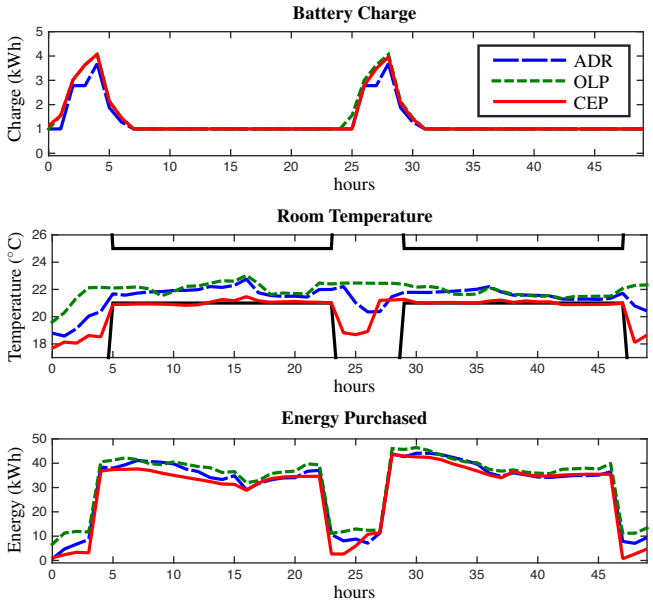

Fig. 2. Profile trajectories for the state of the battery charge (top), room temperature in the first room in building 1 (center), and the total energy purchased from the grid (bottom). The battery charge is calculated as the sum of the two states appearing in (V). The black lines in second graph correspond to the comfort constraint. The uncertain data correspond to the winter period, with the ambient temperature ranging around $5°C$.

horizon, certainty equivalent problem and open-loop policies are solved within 2 second, while affine decision rules require approximate 15 seconds.

To better understand the behaviour of the three approximations, the trajectories for the state of the battery charge, room temperature in the first room in Building 1, and the total energy purchased from the grid $\boldsymbol{p}_t$, are depicted Figure 2. The results verify the behaviour of the three control strategies. Indeed, the certainty equivalent approximation operates very near to the comfort constraint and leads to frequent constraint violations, while the robust approximation produces more conservative results, keeping the room temperature well inside the comfort range at the expense of more energy consumption. All three approximations fully utilize the load shifting capabilities of the battery, storing energy during the evening hours when electricity is cheaper, and deploying that energy in the early morning hours when the building needs to be brought back within the comfort range. From these results, we conclude that the adaptive nature of the affine decision rules produces a good compromise between the optimistic decisions made by the certainty equivalent approximation and the over conservative decisions of the open-loop policies.

VI. Conclusion

In this paper, we presented a unified framework for controlling the operation of the energy hub and the buildings it connects, and formulated a optimization problem that ensures the energy needs of the buildings are met with the minimum cost. We used a decision rule approximation for solving the resulting infinite-dimensional stochastic problem. Our simulations which are based on realistic data have demonstrated that the adaptive nature of the affine decision rules produce a good trade-off between energy consumption and comfort violation compared to established solution techniques.

Future work concentrates on a more comprehensive modeling of the energy hub's dynamics, as well as considering larger building communities connected to the energy hub. From a practical prospective, this will require to investigate the impact of more flexible policies for further reducing the conservativeness of affine decision rules, as well as exploiting the naturally decomposable nature of the problem by implementing distributed and decentralized control schemes.

References

[1] J. Laustsen. Energy efficiency requirements in building codes, energy efficiency policies for new buildings. *International Energy Agency (IEA)*, pages 477–488, 2008.

[2] J. McQuade. A system approach to high performance buildings. Technical report, United Technologies Corporation, 2009.

[3] EN 15251:2007. Indoor environmental input parameters for design and assessment of energy performance of buildings addressing indoor air quality, thermal environment, lighting and acoustics. european committee for standardization, 2007.

[4] M. Maasoumy, M. Razmara, M. Shahbakhti, and A. Vincentelli. Handling model uncertainty in model predictive control for energy efficient buildings. *Energy and Buildings*, 77:377–392, 2014.

[5] F. Oldewurtel, A. Parisio, C. N. Jones, D. Gyalistras, M. Gwerder, V. Stauch, B. Lehmann, and M. Morari. Use of model predictive control and weather forecasts for energy efficient building climate control. *Energy and Buildings*, 45:15–27, 2012.

[6] X. Zhang, S. Grammatico, G. Schildbach, P. Goulart, and J. Lygeros. On the sample size of randomized MPC for chance-constrained systems with application to building climate control. In *European Control Conference (ECC)*, pages 478–483, 2014.

[7] M. Geidl, G. Koeppel, P. Favre-Perrod, B. Klockl, G. Andersson, and K. Frohlich. Energy hubs for the future. *IEEE Power and Energy Magazine*, 5(1):24–30, 2007.

[8] D. Crawley, L. Lawrie, C. Pedersen, and F. Winkelmann. Energy plus: energy simulation program. *ASHRAE journal*, 42(4):49–56, 2000.

[9] R. Evins, K. Orehounig, V. Dorer, and J. Carmeliet. New formulations of the energy hub model to address operational constraints. *Energy*, 73:387–398, 2014.

[10] A. Parisio, C. Del Vecchio, and A. Vaccaro. A robust optimization approach to energy hub management. *International Journal of Electrical Power & Energy Systems*, 42(1):98–104, 2012.

[11] M. Arnold, R.R. Negenborn, G. Andersson, and B. De Schutter. Distributed predictive control for energy hub coordination in coupled electricity and gas networks. In *Intelligent Infrastructures*, pages 235–273. Springer, 2010.

[12] D. Sturzenegger, D. Gyalistras, V. Semeraro, M. Morari, and R. S. Smith. BRCM Matlab Toolbox: Model generation for model predictive building control. In *American Control Conference*, pages 1063–1069, Portland, June 2014.

[13] H. Fakham, P. Degobert, and B. François. Control system and power management for a PV based generation unit including batteries. In *International Aegean Conference on Electrical machines and power electronics, ACEMP'07.*, pages 141–146. IEEE, 2007.

[14] E. I. Vrettos and S. A. Papathanassiou. Operating policy and optimal sizing of a high penetration RES-BESS system for small isolated grids. *IEEE Transactions on Energy Conversion*, 26(3):744–756, 2011.

[15] A. Ben-Tal, A. Goryashko, E. Guslitzer, and A. Nemirovski. Adjustable robust solutions of uncertain linear programs. *Mathematical Programming*, 99(2):351–376, 2004.

[16] A. Georghiou, W. Wiesemann, and D. Kuhn. Generalized decision rule approximations for stochastic programming via liftings. *Mathematical Programming*, pages 1–38, 2014.

[17] D. Sturzenegger, D. Gyalistras, M. Gwerder, C. Sagerschnig, M. Morari, and R. S. Smith. Model predictive control of a Swiss office building. In *11th REHVA World Congress Clima*, 2013.

[18] A. Ben-Tal, L. El Ghaoui, and A. Nemirovski. *Robust Optimization*. Princeton University Press, 2009.